

BRITISH GEOLOGICAL SURVEY
Natural Environment Research Council

TECHNICAL REPORT WD/99/6
Hydrogeology Series

Technical Report WD/99/6

**Development of A Centrifuge Method for the Rapid
Determination of Solvent Pore-entry Pressures**

D C Goody, J P Bloomfield and M Bright

This report was prepared for
EPSRC/NERC

Bibliographic Reference

D C Goody, J P Bloomfield and M Bright, 1999
**Development of A Centrifuge Method for the Rapid
Determination of Solvent Pore-entry Pressures**
British Geological Survey Report WD/99/6



BRITISH GEOLOGICAL SURVEY

BRITISH GEOLOGICAL SURVEY
KEYWORTH
NOTTINGHAM NG12 5GG
UNITED KINGDOM

TEL (0115) 9363100
FAX (0115) 9363200

DOCUMENT TITLE AND AUTHOR LIST

Development of A Centrifuge Method for the Rapid Determination of Solvent Pore-entry Pressures

D C Goody, J P Bloomfield and M Bright

CLIENT EPSRC/NERC Waste and Pollution Management	CLIENT REPORT #
	BGS REPORT# WD/99/6
	CLIENT CONTRACT REF
	BGS PROJECT CODE E83XF001
	CLASSIFICATION OPEN

	SIGNATURE	DATE		SIGNATURE	DATE
PREPARED BY (Lead Author)		11.2.99	CO-AUTHOR		20.4.99
			CO-AUTHOR		11.2.99
PEER REVIEWED BY		20/4/99	CO-AUTHOR		
			CO-AUTHOR		
CHECKED BY (Project Manager or deputy)		20.4.99	CO-AUTHOR		
			CO-AUTHOR		
APPROVED BY (Project Director or senior staff)		20/4/99	CO-AUTHOR		
			CO-AUTHOR		
APPROVED BY (Hydrogeology Group Manager)		28/4/99	OS Copyright acknowledged		
			Assistant Director clearance (if required)		
Layout checked by		21/4/99			

Contents		Page
Tables and Figures		ii
Summary		iii
1.	INTRODUCTION	1
1.1	Terminology	1
1.2	Purpose of Measurements	2
1.3	Determining Capillary Pressure-Saturation Relations Using the Centrifuge Method	3
2.	THEORY	4
2.1	Pore-entry Pressures	4
2.2	Residual Saturation	5
2.3	Capillary Trapping Mechanisms	6
2.4	Principles of the Centrifuge Method	8
3.	EXPERIMENTAL METHOD	10
3.1	Core Preparation and Porosity Measurement	10
3.2	Centrifuge Immiscible Liquid Displacement	10
3.3	Imbibition and Hysteresis Experiment	11
4.	RESULTS	12
5.	DISCUSSION AND CONCLUSIONS	17
6.	REFERENCES	19

Tables and Figures	Page
Table 1. Force per rotation for given core sizes	11
Table 2. Summary of core parameters and centrifuge data	12
Table 3. Correlation matrix for measured parameters	15
Figure 1. Contact angle (measured into water) relations in a) DNAPL-wet and b) water-wet saturated systems (from Wilson et al., 1990)	2
Figure 2. Illustration of capillary trapping by snap-off mechanisms	6
Figure 3. Illustration of capillary trapping mechanisms through by-passing	7
Figure 4. Centrifuge tube assembly for DNAPL displacement of water	9
Figure 5. Pore-entry pressure replication for selected samples	13
Figure 6. Pressure normalised residual saturation cross plots for duplicate samples	14
Figure 7. Pore-entry pressure imbibition and hysteresis	16
Figure 8. Relationship between residual DNAPL and antecedent water saturation	18
Figure 9. Residual DNAPL saturation as a function of mean pore size (μm)	18

SUMMARY

This report details the work carried out to determine the efficacy of a centrifuge method for the determination of dense non-aqueous phase liquid (DNAPL) pore-entry pressures. The aim of the study was to measure solvent pore-entry pressure (and residual saturation) by forcing DNAPL into water saturated sandstone plugs at increasing rotational velocities. It was also an aim of the study to examine any hysteresis effects which may be caused by repeating the process after forcing water back into the cores.

A method was adapted and developed so as to enable the rapid determination of DNAPL pore entry pressures up to an equivalent head of 6 metres of tetrachloroethene or 10 metres of water. The method was shown to be reliable and reproducible and could easily be adapted to a moderately equipped laboratory.

Twenty consolidated sandstone samples were centrifuged, with porosities ranging from 4-34% and permeabilities from 0.005-3000 mD. For these samples the residual water content after centrifuging was found to be between 20 and 100%. Dominant pore-entry pressures varied from 2 to >100 kPa (or 0.1 to > 6m of tetrachloroethene). Good inverse correlations were obtained for residual water saturation and porosity and for dominant pore-entry pressure and porosity.

The method proved difficult to use when trying to quantify imbibition. However, some hysteresis and residual solvent saturation was found after the water imbibition experiment was carried out. When DNAPL was flooded back into the core very similar final residual water concentrations were found for the same samples. It has been inferred from this that in a spill-scenario the residual saturation in the saturated zone will not exceed the maximum after the first DNAPL flood.

A relationship has also been established between residual DNAPL saturation and initial water saturation, with a trend of decreasing residual DNAPL saturation for increasing water saturation. A tentative relationship between mean pore size (as calculated from MICP data) and residual DNAPL saturation has also been proposed. The relationship implies that for realistic environmental loadings residual DNAPL saturation will not reach 100% for the mean pore sizes in consolidated sandstone media.

1. INTRODUCTION

The term 'non-aqueous phase liquid (NAPL)' is used to describe an organic liquid that will only dissolve sparingly in water. NAPLs are typically divided into two categories, denser than water ('sinkers') and less dense than water ('floaters'). The halogenated solvents belong to the former group and are called dense non-aqueous phase liquids (DNAPLs). These compounds possess physicochemical properties which make them extremely insidious groundwater contaminants (Aurang et al, 1981).

Where a spillage of DNAPL is sufficiently large that the residual saturation capacity of the unsaturated zone is exceeded then it will reach the water table and contaminate the aquifer directly. In the saturated zone, DNAPL migration occurs only when the pressure exerted by its greater density is able to overcome the pore-entry pressure of the rock. There are several major factors influencing solvent pore-entry pressure and residual saturation and these are detailed below.

1.1 Terminology

Interfacial tension

In the interior of a homogeneous fluid, a molecule is surrounded on all sides by other molecules exerting cohesive forces between one another. At the interface between two immiscible fluids however, there are few if any like molecules across the interface. A molecule at the interface is attracted to molecules of its own phase by a force greater than the force attracting it to molecules of the 'immiscible' phase across the interface. This unbalanced force draws molecules along the interface inward and results in the tendency for the fluid-fluid interface to contract. If the interface is stretched, it acts like an elastic membrane. The restoring force seeking to minimize the interfacial area between the two immiscible fluids, is called the interfacial tension, σ . When encountered between a liquid and a gas, this same force is called the surface tension, λ .

Contact angle

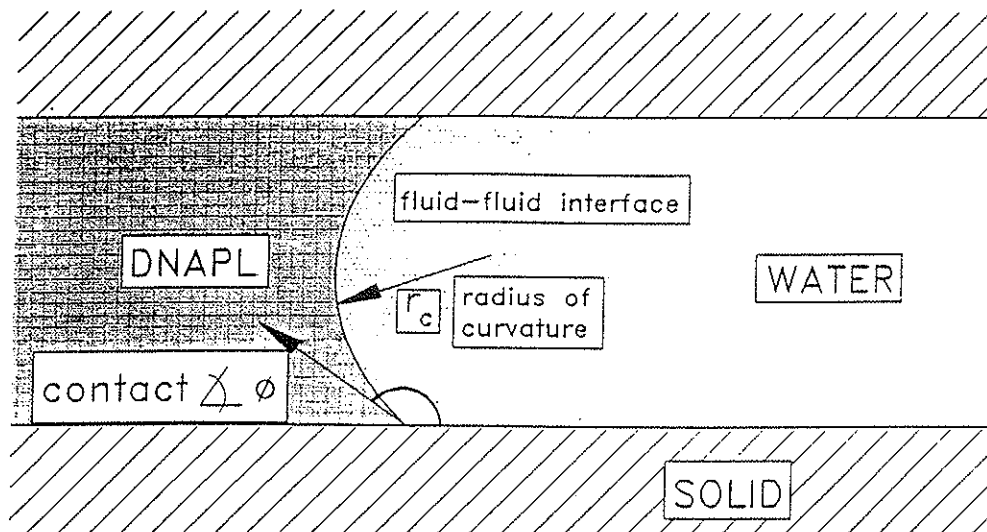
For a system of two immiscible fluids (eg water and organic liquid) in contact with a solid phase both the cohesive forces within the fluids and the adhesive forces between the solid and each of the fluids are at work at the line of contact. If the adhesive forces between the solid and the water phase are greater than the cohesive forces inside the water itself and greater than the forces of attraction between the organic phase and the solid, then the solid-water contact angle, θ , will be acute and the water will 'wet' the solid (see Figure 1). Most saturated media are preferentially wet by water. The contact angle provides the only direct measurement of wettability but is a difficult measurement to make under laboratory conditions without compromising the integrity of true environmental conditions.

Capillarity

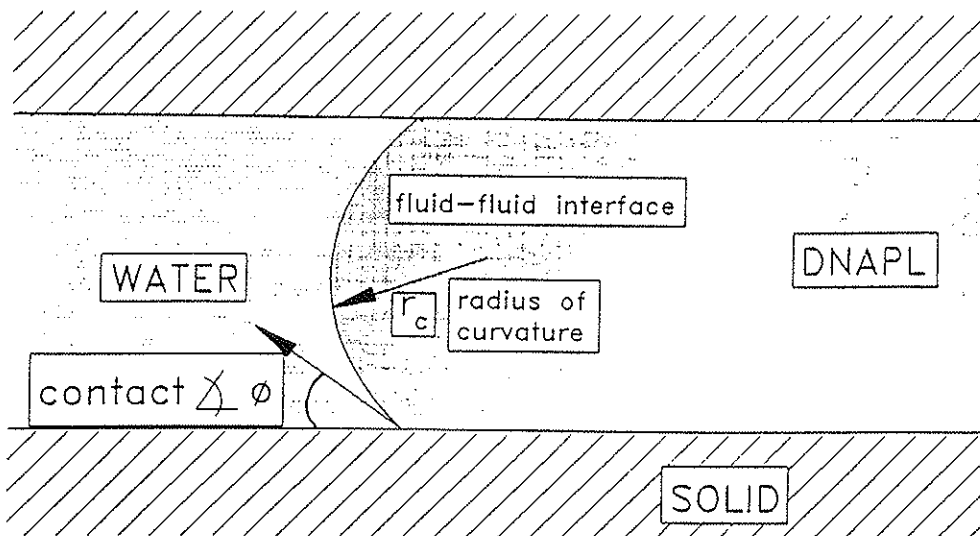
As a result of the contact angle, a meniscus is formed between the fluid phases. As tubes (or capillaries) get narrower the radius of curvature between the two immiscible phases gets smaller. Similar to the curvature produced by a pressure difference across a membrane, the presence of curvature implies a pressure difference across the fluid-fluid interface, called the capillary pressure.

Capillary Pressure

Capillary pressure causes porous media to draw in the wetting fluid and repel the nonwetting fluid due to the dominant adhesive force between the wetting fluid and the media solid surfaces. For a water-NAPL system with water being the wetting phase as in an aquifer, capillary pressure equals the NAPL pressure minus the water pressure.



(a) contact $\Delta \phi > 110^\circ$: DNAPL WET



(b) contact $\Delta \phi < 70^\circ$: WATER WET

Figure 1. Contact angle (measured into water) relations in a) DNAPL-wet and b) water-wet saturated systems (from Wilson et al., 1990)

1.2 Purpose of Measurements

Capillary pressure measurements are essential for the complete characterisation of an oil reservoir. They are also essential for determining the degree of penetration likely to occur in an aquifer system after the spillage of a dense non-aqueous phase liquid (DNAPL). A plot of capillary pressure against saturation for a rock core, called the capillary pressure curve, may be a useful way of estimating the potential risk to groundwater from any given DNAPL spill incident. These curves also provide data on the irreducible water saturation and the entry pressure of LNAPL or DNAPL into a water-saturated reservoir.

Two main types of methods are available to determine capillary pressure-saturation $P_c(S_w)$ relations in porous media, i) displacement methods based on establishing successive states of hydraulic equilibrium and ii) dynamic methods based on establishing successive rates of steady flow of wetting and non-wetting fluids. Displacement methods are utilized more commonly than dynamic methods.

1.3 Determining Capillary Pressure-Saturation Relations Using the Centrifuge Method

Three static (non-flow) methods of obtaining capillary pressure curves are the porous plate, mercury injection, and centrifuge methods. The centrifuge method compares favourably with the other methods of preparing capillary pressure curves. The porous plate method may require weeks whereas the centrifuge can take only days. Any fluid combination (gas-oil, gas-water, water-LNAPL, Water-DNAPL, gas-water-LNAPL, gas-water-DNAPL) can be used in the centrifuge. The centrifuge method is non-destructive and the results are reproducible. Both drainage and imbibition curves can be produced. Interphase differences up to 7 MPa can be developed in an air-liquid system, extending the range of permeability down to one millidarcy (md) or less. Unconsolidated samples can be evaluated on the centrifuge.

The seminal work on the centrifuge method was by Hassler and Brunner (1945). Slobod and Chambers (1951) demonstrated the simplicity, reproducibility and speed in the centrifuge method, and its good correlation with the porous plate method. They also indicated the very high pressure differences between the phases. Marx (1956) discussed the use of the centrifuge in a gravity drainage investigation. Hoffman (1963) performed dynamic (time-dependant) measurements of saturation in core samples using a constantly accelerating centrifuge, with considerable time savings. Donaldson et al (1969) used the centrifuge for capillary pressure measurements in a study of wettability. Szabo (1970) extended the method to include imbibition capillary pressure curves. He also used the centrifuge to measure electrical resistivity as a function of saturation. Samaroo and Guerrero (1981) used a centrifuge to measure the effects of temperature on drainage capillary curves. Hagoort (1980) and Van Spronsen (1982) have both used the centrifuge to make two- and three-phase relative permeability measurements. More recently researchers have been focusing on using ultracentrifuges to obtain higher quality continuous data and to improve iterative methods for calculating capillary pressure curves (Ruth and Wong, 1990; Kantzas et al, 1995; Nikakhtar et al, 1996). Kinniburgh and Miles (1983) used immiscible fluid displacement of water from consolidated and unconsolidated media by using the centrifuge but were not interested in investigating pore-entry pressure relationships. As yet the centrifuge has not been used to measure pore-entry pressure for solvents in consolidated media.

2. THEORY

2.1 Pore-entry Pressures

In hydraulic systems, threshold entry pressure into a porous media can be estimated as an equivalent head of water by

$$h_c = (2 \sigma \cos \phi) / (r \rho_w g) \quad (1)$$

where h_c is the capillary rise of the wetting fluid (water), ρ_w is the density of water, and g is acceleration due to gravity. Similarly, the critical DNAPL thickness, z_n required for DNAPL penetration into water saturated pores with radii r , can be estimated by

$$z_n = (2 \sigma \cos \phi) / [r g (\rho_n - \rho_w)] \quad (2)$$

where ρ_n is the DNAPL density.

Under hydrostatic conditions, the potential for DNAPL penetration of progressively finer pore openings increases proportionally to the overlying DNAPL column thickness and the DNAPL-water density difference. Once DNAPL enters a vertical fracture, it will readily invade finer and finer fractures with depth due to the increase in DNAPL height with fracture depth. In natural media, pore spaces are extremely complex and irregular, and their geometry can not be described analytically (Bear, 1988). Due to their variability, the threshold entry pressure for each pore will be different.

The equation

$$P_c = (2 \sigma \cos \phi) / r \quad (3)$$

implies that the wetting phase will be progressively displaced from larger to smaller pores by the nonwetting phase with increases in nonwetting NAPL pressure head and that the capillary entry pressure is driven by pore size distribution and fluid interfacial tensions (Parker, 1989). Laboratory experiments demonstrate that capillary pressure can be represented as a function of saturation. PCE-water drainage capillary pressure-saturation curves were determined for several sands of varying hydraulic conductivity by Keuper and Frind (1991). The capillary pressure curve is typically L-shaped with a low threshold entry pressure for coarser-grained, higher permeability materials and a higher threshold entry pressure for finer-grained, lower permeability materials. DNAPL saturation increases with capillary pressure because higher capillary pressures are required to displace water from incrementally smaller pore openings.

To enable modelling of these data, laboratory $P_c(S_w)$ measurements are often fitted by a non-linear regression using an empirical parametric model such as the Brooks-Corey (1964) or the van Genuchten models (1980).

The Brooks-Corey $P_c(S_w)$ relationship states

$$S_e = (P_c/P_d)^\lambda \quad (4)$$

where $S_e = (S_w - S_{wr}) / (1 - S_{wr})$, S_w is the water saturation, S_{wr} is the residual water saturation, P_d is the threshold entry pressure of the medium corresponding to the nonwetting phase entry, and λ is a pore-size distribution index.

2.2 Residual Saturation

During migration, a significant portion of NAPL is retained in porous media, thereby depleting and eventually exhausting the mobile NAPL body. Below the water table, residual saturation (S_r) of NAPL is the saturation ($V_{\text{NAPL}}/V_{\text{voids}}$) at which NAPL is immobilised (trapped) by capillary forces as discontinuous ganglia under ambient groundwater flow conditions. In the unsaturated zone, however, residual NAPL may be more or less continuous depending on the extent to which NAPL films develop between the water and gas phases thereby interconnecting isolated NAPL blobs (Wilson et al., 1990). The physics of entrapment and development of methods to minimize residual saturation by enhanced oil recovery (EOR) are of great economic importance to the oil industry. Similarly, residual saturation has important consequences in the migration and remediation of subsurface NAPL. Residual saturation for the wetting fluid is conceptually different from that for the nonwetting fluid. The nonwetting fluid is discontinuous at residual saturation, whereas the wetting fluid is not.

In the unsaturated zone, NAPL is retained as films, wetting pendular rings, wedges surrounding aqueous pendular rings, and as nonwetting blobs in pore throats and bodies in the presence of water. NAPL will spread as a film between the water and gas phases given a positive spreading coefficient:

$$\Sigma = \sigma_{\text{sw}} - (\sigma_{\text{nw}} + \sigma_{\text{an}}) \quad (5)$$

where Σ is the spreading coefficient, σ_{sw} is the interfacial tension for air-water, σ_{nw} is the interfacial tension for NAPL-water, and σ_{an} is the interfacial tension for air-NAPL. DNAPLs such as halogenated solvents typically have negative spreading coefficients and will not spread as films in the unsaturated zone due to their internal cohesion.

Based on laboratory determinations using various NAPLs and saturated soils, Wilson et al. (1990) found that residual saturation could not be reliably predicted from soil texture because very minor textural differences, such as the inclusion of trace silt or clay in sand, and the presence of heterogeneities significantly affect residual saturation values. For a given NAPL release volume, residual saturation in fractures and macropores tend to be less than in homogeneous porous media but can be expected to extend over a larger portion of the aquifer. In addition residual saturation in heterogeneous media containing discontinuous coarse lenses tends to be greater than in homogeneous media, but can be expected to extend over a smaller portion of the aquifer.

To determine the potential residual saturation for a particular porous medium, Wilson et al (1990) recommend that site specific residual saturation measurements be made using an ideal fluid having a sufficient density difference with water, low solubility, low volatility, and low toxicity rather than the site-specific NAPL (except if some unusual wetting behaviour or NAPL dependent interactions between phases is expected). Under low capillary number and Bond number conditions, S_r values are relatively insensitive to fluid properties. The Bond number represents the ratio of gravitational forces to viscous forces that affect fluid trapping and mobilisation. It can be given as a dimensionless number such that:

$$N_b = \Delta\rho g r^2 / \sigma \quad (6)$$

where $\Delta\rho$ is the fluid-fluid density difference, g is gravitational acceleration, r is a representative grain radius, and σ is the fluid-fluid interfacial tension. For soils with a wide grain size distribution, r can be replaced by intrinsic permeability. The capillary number represents the ratio of viscous forces to capillary forces that affect fluid trapping and mobilisation. It can be given as:

$$N_c = k i_w / \sigma \quad (7)$$

where k is the intrinsic permeability, i_w is the water phase pressure gradient, and σ is the fluid-fluid interfacial tension.

A residual source may contaminate groundwater for decades because drinking water standards for many NAPLs are orders of magnitude less than their solubility limits. Water can be contaminated by direct dissolution of residual NAPL and/or by contact with soil gas containing NAPL volatiles from a residual source in the unsaturated zone. Combined with the practical limitations on residual NAPL recovery, the consequences of NAPL dissolution may necessitate perpetual hydraulic containment at some sites. Unless residual NAPL is replenished by continued contaminant release or unusual hydraulic conditions, it will tend to be slowly diminished by dissolution, volatilisation and in some cases biodegradation. At some sites, remediation may involve partial mobilization of residual saturation by increasing the prevailing hydraulic gradient or reducing interfacial tension.

2.3 Capillary Trapping Mechanisms

When two fluid phases are present, and the non-wetting fluid is being displaced by the wetting fluid as in the hysteresis study, there are two major mechanisms for capillary trapping: snap-off and by-passing.

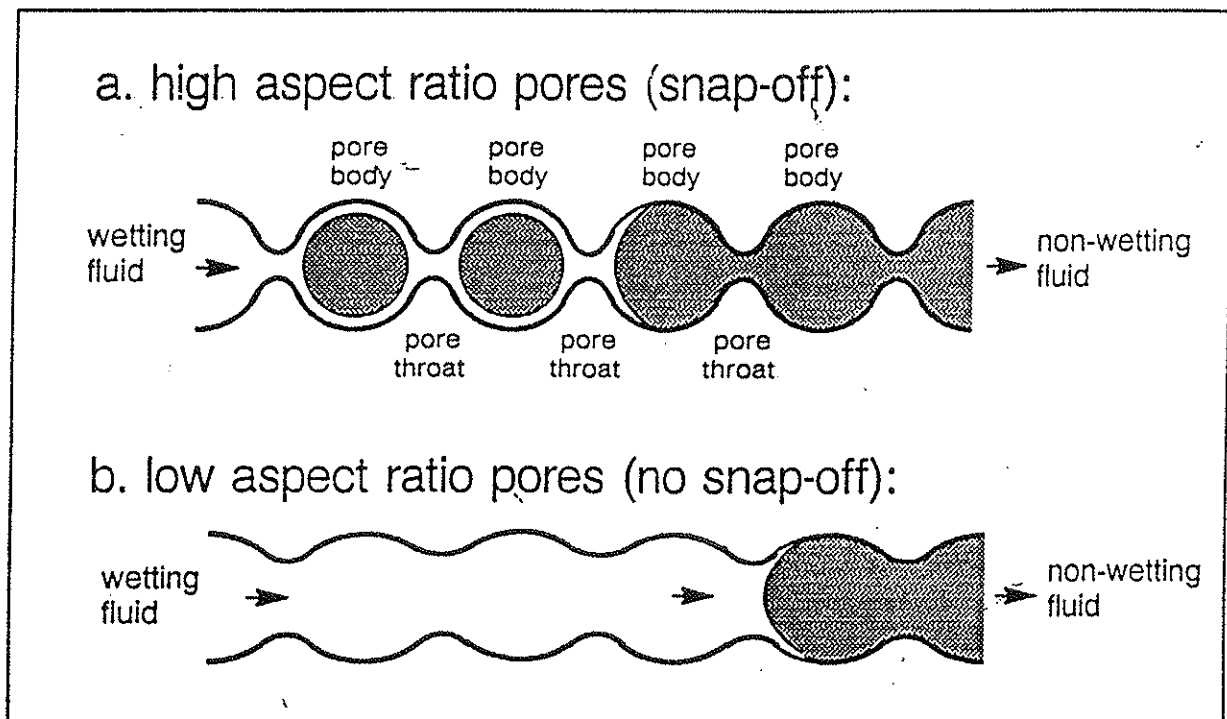


Figure 2. Illustration of capillary trapping by snap-off mechanisms.

Snap-off occurs as non-wetting fluid in a pore is displaced from a pore body into a pore throat. The mechanism strongly depends on wettability and the aspect ratio (the ratio of pore-body diameter to pore-throat diameter). For low aspect ratio pores (Figure 2), in which the pore throats are almost as large as the pore bodies, the non-wetting fluid can be completely displaced and no snap-off occurs. However, in high aspect ratio pores, the pore throats are much smaller than the pore bodies and when a thin layer of wetting phase reaches the exit pore throat, a large blob of non-wetting phase still remains in the pore. Snap-off occurs as the wetting phase continues through the exit throat leaving behind the now disconnected blob. The trapping is a function of wetting and contact angle as well as pore geometry. The combined effect of

contact angle and pore geometry control the curvature of a fluid-fluid interface and determine the potential for snap-off.

The mechanism of 'by-passing' is commonly described with reference to the concept of a 'pore doublet'. A pore doublet consists of a tube which splits into two pores, one generally narrower than the other, and then rejoins (Figure 3).

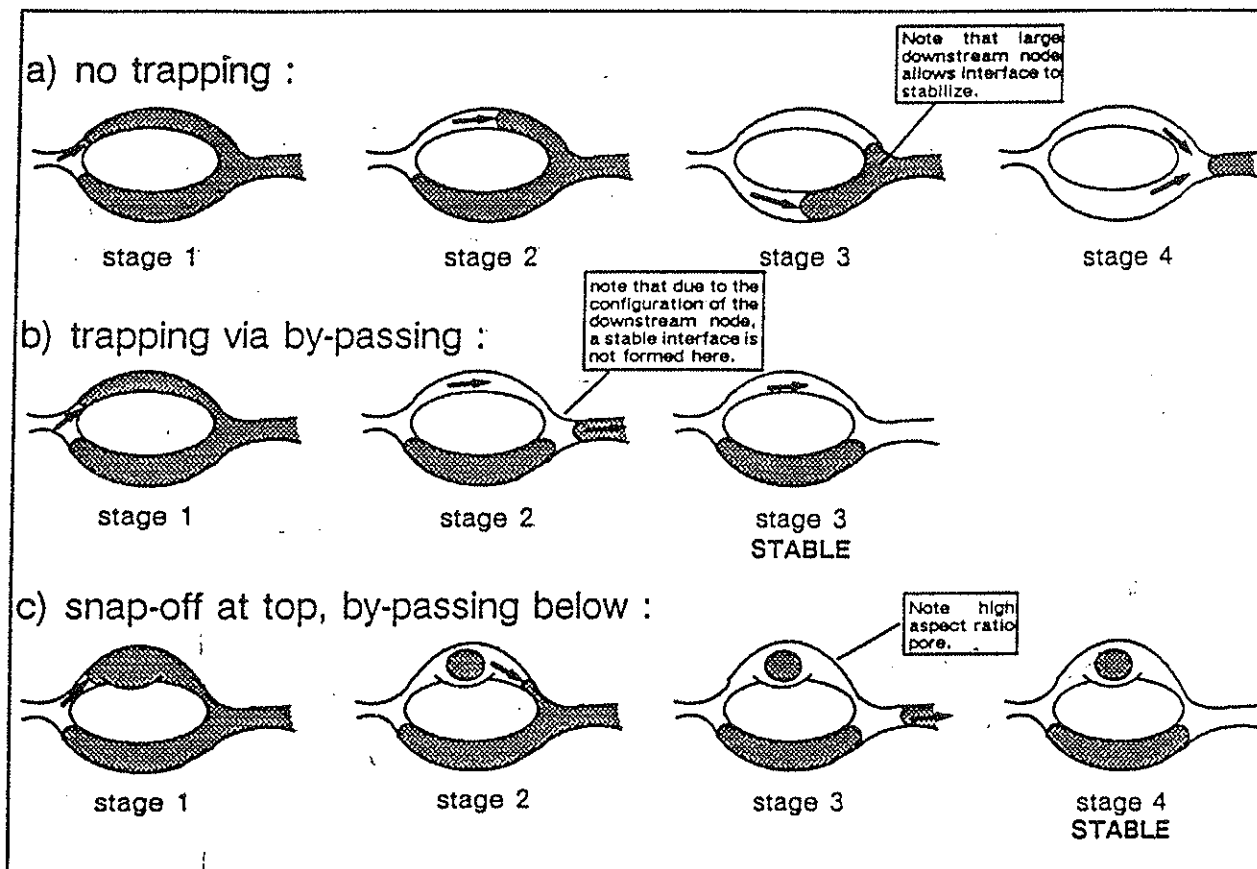


Figure 3. Illustration of capillary trapping mechanisms through by-passing

No trapping of a non-wetting organic phase occurs when the advancing wetting phase enters the narrower pore opening first (Figure 3a). In each pore, the total pressure drop driving flow is the sum of the capillary pressure and the dynamic pressure drop caused by flow. For the pore doublet to have any physical meaning, the flow rates (and dynamic pressure drop) should be low enough to approximate aquifer conditions. On a pore scale, under such conditions, capillary forces are much larger than the dynamic viscous forces. Capillarity thus controls the advance of the wetting front (water), causing wetting fluid to fill the narrower pore. The water-organic interface remains stable at the entrance to the wider pore. When the wetting phase reaches the downstream node (where the pores rejoin), it forms a stable meniscus with the non-wetting phase because the cross-section at the downstream node is greater than at the entrance to the wider pore. In instances where a stable meniscus can be maintained at the downstream node, the wetting fluid can then push non-wetting fluid out of the wider pore. If the menisci can rejoin at the downstream node, the water has displaced the organic liquid completely from the pore doublet and no trapping has occurred.

In the by-passing mechanism of trapping, the water enters the narrower pore first as before, however as water reaches the downstream node (Figure 3b), it does not stop because no stable interface is formed. The

organic liquid in the wider pore has become disconnected from the main body of organic liquid and is unable to drain from the pore. The liquid has become ‘by-passed’ by the advancing water.

Snap-off and by-passing trapping can both occur in the pore doublet (Figure 3c). Water again enters the narrower pore initially but due to the high aspect ratio in the pore, snap-off occurs. Water then continues to move through the narrower pore and through the down stream node. No stable meniscus is formed and organic liquid in the wider pore is by-passed.

The pore doublet model allows the organic liquid to be by-passed in at most one pore. However, in a porous medium the organic phase in several pores may be collectively by-passed leaving an organic blob which extends over several pores. In contrast, blobs trapped by snap-off extend over one pore only. As pore aspect ratio decreases, the proportion of organic liquid trapped by by-passing, relative to snap-off, increases, and blobs become larger and more complex.

2.4 Principles of the Centrifuge Method

At hydrostatic equilibrium the capillary pressure at every position is equivalent to the difference in hydrostatic pressure between the phases, i.e.

$$P_c(r) = \frac{1}{2} \Delta\rho\omega^2 (r_c^2 - r^2) \quad (8)$$

where: r represents the distance from the centre of rotation, r_c represents the radius of the core bottom, $\Delta\rho$ represents the difference between the density of the phases, and ω the rate of rotation in radians per second. For each value of $P_c(r)$ there is a corresponding value of water saturation $S_w(r)$ at each radial position r , and both may vary substantially from one end of the core to the other. The essential problem that must be solved to get a capillary pressure curve is to relate P_c to its appropriate S_w .

A method for doing this has been suggested by Hassler and Brunner (1945). They computed capillary pressure and saturation at the top face of the core ($r = r_i$). They state

$$P_c(r_i) = z = \frac{1}{2} \Delta\rho\omega^2 (r_c^2 - r_i^2) \quad (9)$$

and

$$S_w(r_i) = S_w(z) \quad (10)$$

The water saturation at the top of the face of the core is obtained from the relation

$$S_w(z) = \frac{d}{dz} [z \overline{S_w}(z)] \quad (11)$$

Hassler and Brunner indicate that this is actually an approximation on the correct value for $S_w(z)$, accurate enough for $r_i/r_c \geq 0.70$, and proposed an iterative technique to improve the approximation, which is not discussed further here.

The Hassler-Brunner theory rests on several assumptions that should be kept in mind whenever interpreting data. The model is one-dimensional. Centrifugal acceleration and fluid flow are assumed to be parallel to the axis of the core. The assumption that $S_w = 100\%$ at $r = r_c$ is necessary, and the theory is based on the ‘bundle of capillary tubes’ model of the porous medium.

The bundle of capillary tubes model is the simplest possible model of pore structure for capillary pressure purposes. It assumes a bundle of cylindrical capillary tubes of different diameters and equal lengths, where every capillary has a uniform diameter along its entire length. The drainage capillary pressure curve can be interpreted in terms of this simple model by postulating that at the threshold capillary pressure of penetration of the nonwetting fluid, the largest capillary gets penetrated and filled, and at increasing capillary pressures, increasingly smaller tubes become filled. It is evident that this simple model is incapable of accounting for capillary hysteresis and for the existence of irreducible wetting and residual nonwetting phase saturation.

In the experimental method described in section 3, a fully water saturated core sample is placed in a centrifuge tube in a holder in a centrifuge rotor. The centrifuge tube is then filled with DNAPL so as to completely immerse the core when the core is in a horizontal plane (see Figure 4). This arrangement permits the measurement of volumes of water expelled from the core and replaced by DNAPL in the pore spaces. Water, by definition, is less dense than a DNAPL, so when it is expelled from the pore it floats to the top of the DNAPL in the centrifuge tube. The first data point is obtained at a low centrifugal field by selecting a low rate of rotation. The expelled water volume is measured until it no longer changes. The volume of water remaining in the core is divided by the core's total pore volume to give an average water saturation value, \bar{S}_w . Subsequent points are obtained by a series of increasing rates of rotation.

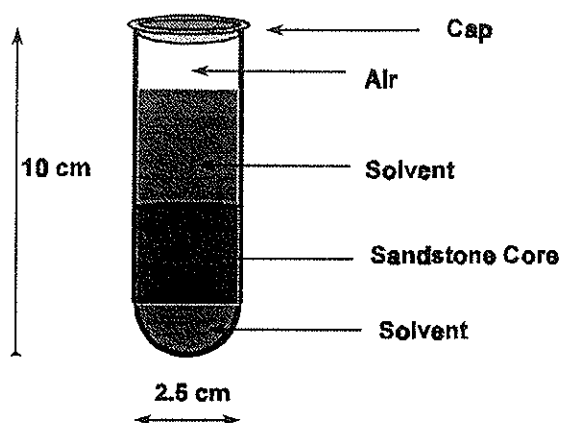


Figure 4. Centrifuge tube assembly for DNAPL displacement of water

3. EXPERIMENTAL METHOD

3.1 Core Preparation and Porosity Measurement

Right-cylindrical plugs of ca. 24.5 mm in diameter and ca. 27.5 mm in length are prepared and oven dried at 60°C for 24 hours prior to testing. Samples are dried to enable a vacuum to be established prior to sample saturation. A sample to be tested is weighed and then placed in a resaturation desiccator. The desiccator is evacuated for at least 24 hours before being flooded with water. The sample is then allowed to saturate for at least a further 24 hours. The saturated sample is then weighed, firstly below the water and then, still saturated with water, in air. For each sample its dry weight, saturated weight under water and its saturated weight in air are recorded, in addition the density of the water is noted. From these values sample dry bulk density, grain density and interconnected porosity can be calculated as follows:

$$\rho_b = \frac{(w\rho_f)}{(S_1 - S_2)} \quad (g \text{ cm}^{-3}) \quad (12)$$

where:

w	=	dry sample weight (g)
S ₁	=	saturated sample weight in air (g)
S ₂	=	saturated sample weight under water (g)

$$\rho_g = \frac{(w\rho_f)}{(w - S_2)} \quad (g \text{ cm}^{-3}) \quad (13)$$

$$\phi = \frac{(S_1 - w)}{(S_1 - S_2)} \times 100 \quad (14)$$

ρ_b	=	dry bulk density (g cm ⁻³)
ρ_g	=	grain density (g cm ⁻³)
ϕ	=	effective porosity (%)
ρ_f	=	density of water (g cm ⁻³)

The effective error of the technique, based on previous repeatability tests, is estimated to be approximately ± 0.5 porosity percent.

3.2 Centrifuge Immiscible Liquid Displacement

The 100% water-saturated cores were placed in Nalgene test tubes and approximately 30 ml of tetrachloroethene was added to each tube prior to loading in a Centaur 2 Centrifuge fitted with a 4-place swing-out rotor. The run began at the lowest speed, 100 rpm.

The rotation rate was held constant for 90 minutes. The centrifuge was then stopped and the displaced water removed with a glass pipette and placed in a 1mL burette with 0.01 mL divisions for accurate

measurement. The centrifuge was then restarted and run for a further 30 minutes. This process was repeated until no further water was eluted from any of the cores. For a given driving force, most water was completely eluted within 180 minutes.

The rotor head speed was increased to a maximum of 2800 rpm. The force on the sample mid-point for a 35, 30 and 25 mm long core is shown in the table below. This final velocity was chosen as it is equivalent of a head of solvent (PCE) of around 5-6.5 m. Some low permeability samples were tested up to 20000 rpm on a high speed centrifuge, an equivalent head of 180 m of PCE. Many samples began to degrade and ultimately disintegrate when taken beyond 3500 rpm (roughly 10 m of PCE).

Table 1. Force per rotation: for given core sizes.

Rotation (rpm)	35 mm	30 mm	25 mm
	Force (kPa)		
100	0.13	0.12	0.10
200	0.54	0.48	0.41
300	1.21	1.07	0.92
400	2.15	1.90	1.64
500	3.36	2.97	2.55
600	4.84	4.28	3.68
800	8.60	7.61	6.54
1000	13.4	11.9	10.2
1200	19.4	17.1	14.7
1500	30.2	26.8	23.0
2000	53.8	47.6	40.9
2500	84.0	74.3	63.9
2800	105	93.2	80.1

3.3 Imbibition and Hysteresis Experiment

Three cores were selected for an imbibition experiment. After the first complete solvent centrifuge run up to 2800 rpm, the cores were removed from the DNAPL, weighed and then centrifuged again with water as the displacing agent. Since the cores were still water wet the water almost spontaneously imbibed displacing the DNAPL to the bottom of the centrifuge tubes. This made measurement of the expelled solvent very difficult and eventually quantifiable measurement of the liquid was abandoned in favour of weighing the whole core sample. For this reason the imbibition curves were not obtained. The weight of the core after centrifuging at 2800 rpm was taken as the final weight and used to calculate solvent residual saturation.

After the imbibition step the water was replaced by DNAPL and the experiment repeated in DNAPL displacement mode with the water displaced again measured volumetrically.

4. RESULTS

Plots for the duplicate data have been shown in Figure 5. These show:

- i) Cumulative volume of water extracted against rotational speed
- ii) Pressure against residual saturation
- iii) Volume against pressure.

The duplicates show good agreement. When normalised for pressure (ie the cores are of different length so a given rotational velocity produces a slightly different pressure on the rock) and plotted against each other (Figure 6) the ratios are close to parity and regressions are all excellent. It can be seen that the greatest variation is for sample 1524/4V which deviates from unity by 17%. Sample 1526/4V varies by just 7% and Sample 1530/8V deviates from unity by just 3%. The agreement between duplicates has improved with time as greater skill and confidence in using the equipment and method has been gained.

The results for all samples have been summarised in the table below. The term PEP_i is used is the pore entry pressure at which solvent displaces the maximum volume of water from the core.

Table 2. Summary of core parameters and centrifuge data

Sample	Porosity (%)	Permeability (mD)	PEP_i (kPa)	S_w
1524/3v	34.3	2324	3.4	0.38
1524/4v	28.6	157	8.5	0.52
1524/4v/2	28.4	143	7.3	0.46
1525/5v	29.3	339	6.5	0.45
1525/6v	32.9	2066	3.4	0.41
1526/4v	28.4	471	4.8	0.47
1526/4v/2	27.8	379	4.5	0.51
1526/6v/2	29.2	439	4.1	0.43
1526/10v	25.7	29.51	9.1	0.52
1527/1v	5.5	0.005	>100	1.00
1527/5v	6.8	0.006	>100	1.00
1527/5v/2	7.1	0.005	>100	1.00
1527/8v/2	4.1	0.007	>100	1.00
1528/2v	21.0	383	8.5	0.46
1529/1v/2	17.3	344	2.0	0.41
1529/6v	23.1	130	4.9	0.49
1529/6v/2	23.4	144	4.6	0.41
1530/8v	24.6	2676	2.1	0.39
1530/8v/2	24.5	2896	2.1	0.35
1530/10v	23.1	2231	2.4	0.19

A correlation matrix for all 20 samples centrifuged is presented below.

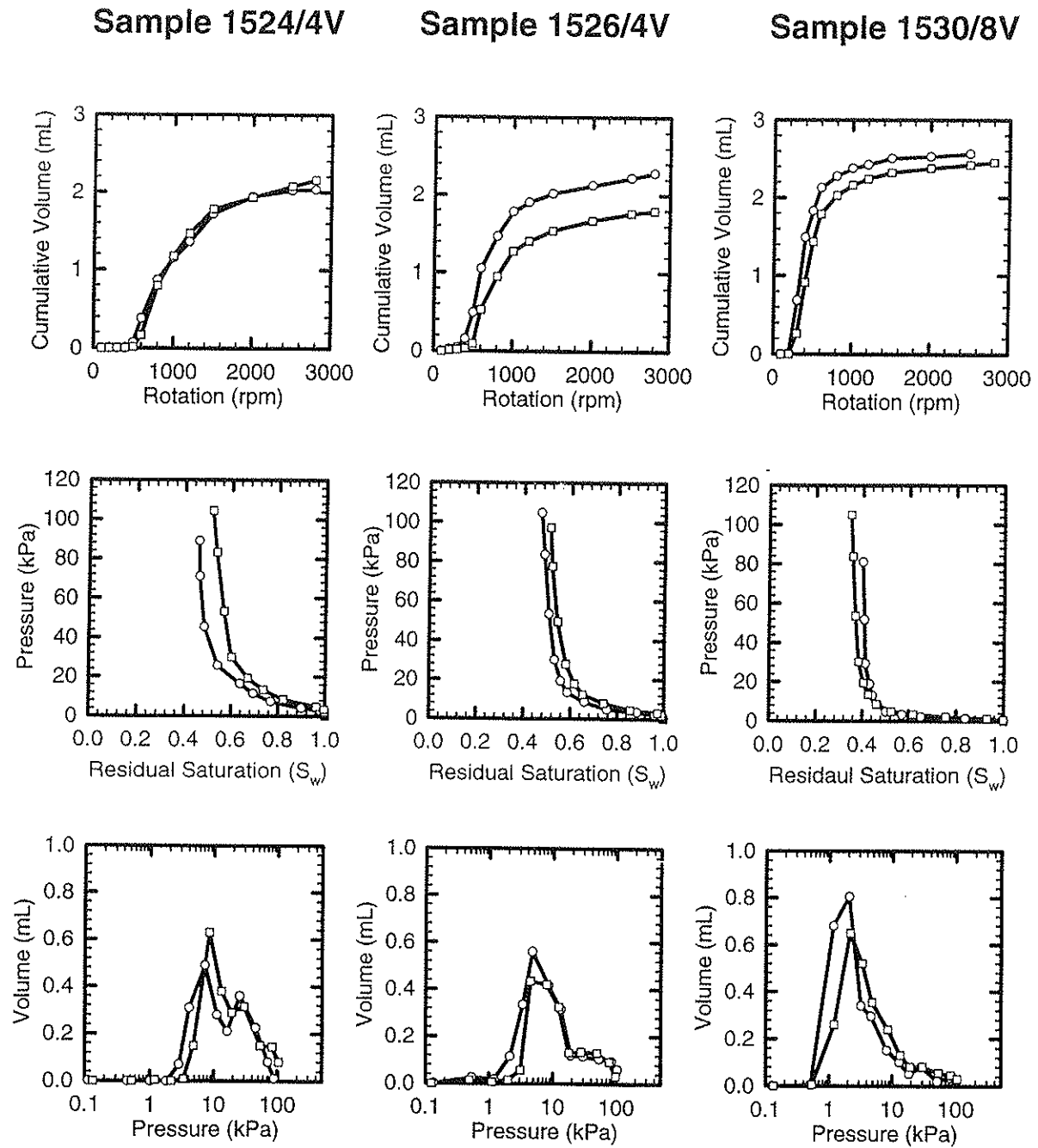
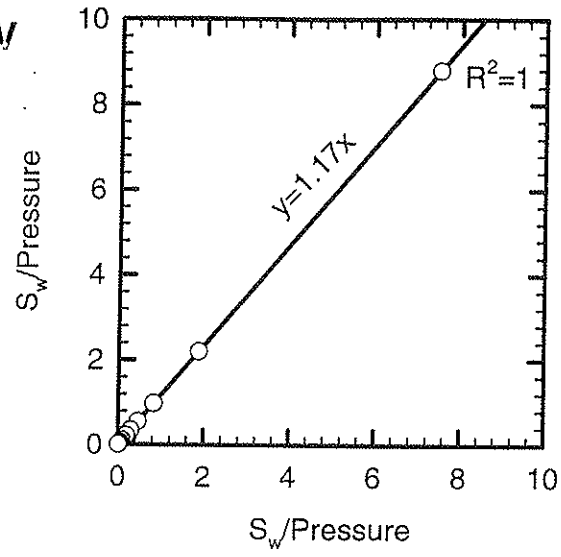
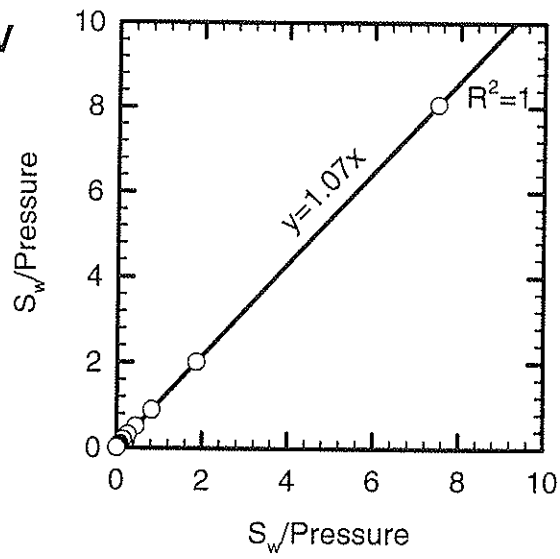


Figure 5. Pore-entry pressure replication for selected samples

Sample 1524/4V



Sample 1526/4V



Sample 1530/8V

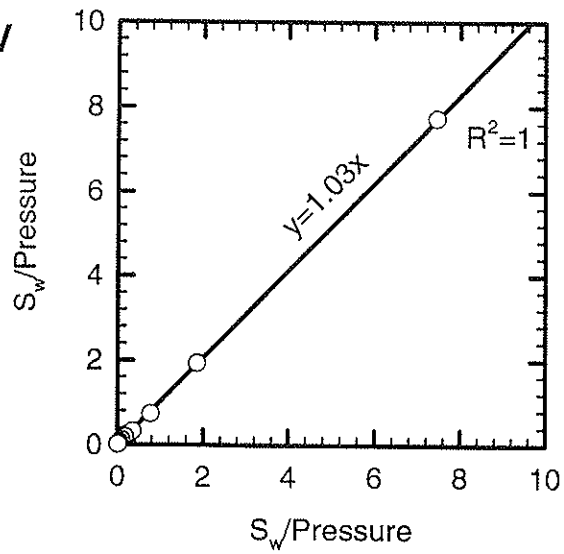


Figure 6. Pressure normalised residual saturation cross plots for duplicate samples

Table 3. Correlation matrix for measured parameters

	Porosity	Permeability	PEP_i	S_w
Porosity	1			
Permeability	0.42	1		
PEP_i	-0.87	-0.38	1	
S_w	-0.84	-0.53	0.94	1

Table 3 demonstrates that both residual water saturation and the initial pore-entry pressure are strongly related to the porosity. High porosities correspond to low residual water saturations and vice-versa.

The imbibition and hysteresis experiments are shown in Figure 7. Only the two water drainage (DNAPL penetration) curves are shown. The difference between the starting point of the first and second curve is the residual saturation of DNAPL.

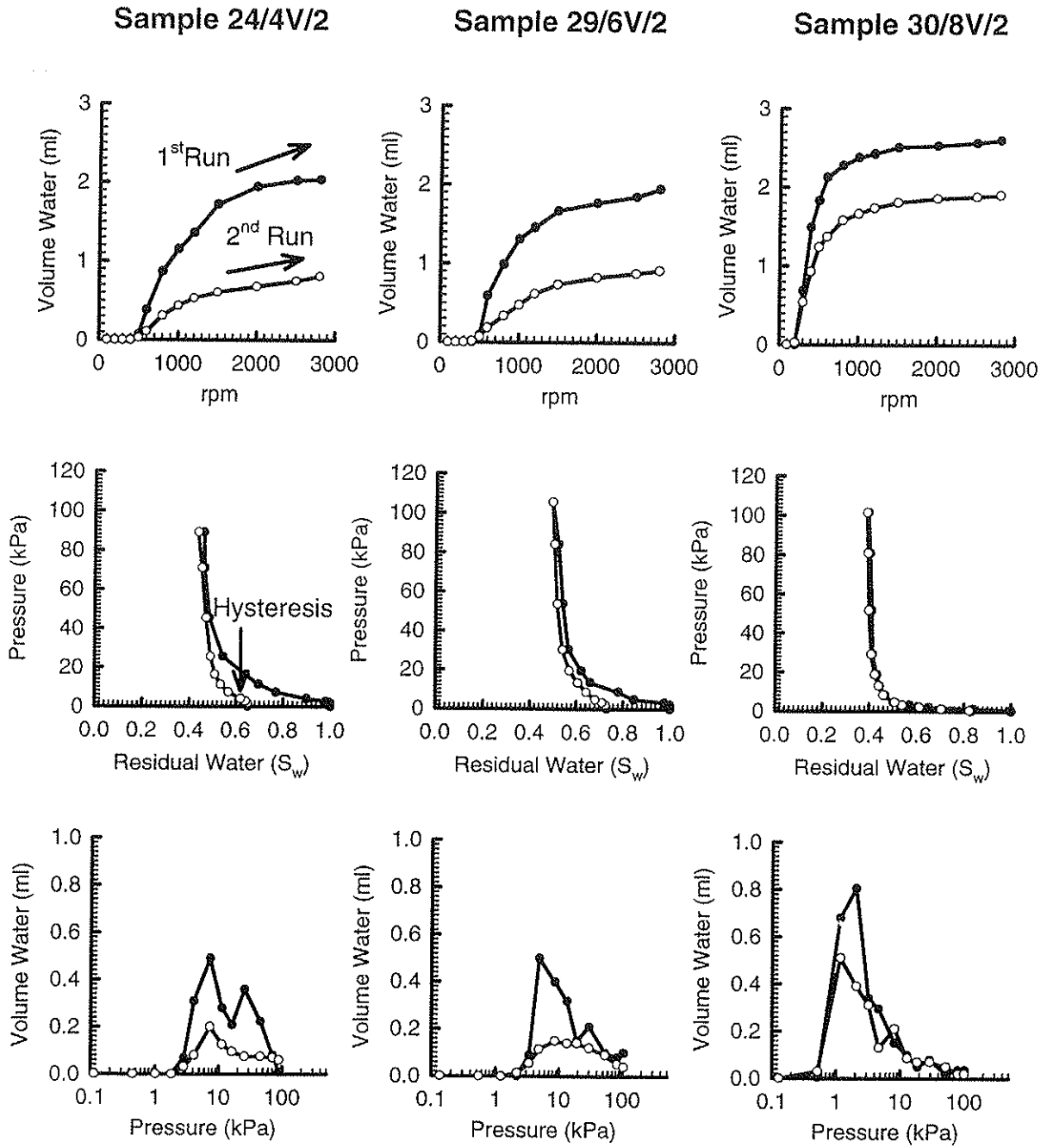


Figure 7. Pore-entry pressure imbibition and hysteresis

5. DISCUSSION AND CONCLUSIONS

On a practical level it is essential that clean glass pipettes are used for each water sample and that the glass burettes are thoroughly cleaned and dried in between measuring volumes of water expelled. Failure to do this results in the loss of water as it becomes attached to burette and pipette walls and an underestimation as to the true volume of water, hence an overall underestimate as to the residual DNAPL saturation. In the narrow capillary tubes used small pockets of water were found to be easily trapped under layers of DNAPL if the glassware was in any way dirty.

The stopping and starting of the centrifuge may lead to some redistribution of the water and DNAPL in between successive centrifuge runs. The net effect of this redistribution may be reduced DNAPL residual saturations as water is still the wetting phase and so may displace DNAPL. It is considered however that this effect may be relatively minor and this is supported by the duplicate sample runs.

The method also produces a gradient of force across the core plug. The force at the top of the core can be at least 50% greater than that at the cores mid-point. There is no way to easily avoid this problem, even if the centrifuge speed could be incremented continuously and smoothly there would still be a gradient of force and the absolute pressure across the plug would still be an integral.

Grain loss during the DNAPL flooding stage was a minor problem. Due to the loading of the force around the base of the core, some sand grains are displaced hence ending up in the base of the centrifuge tube. This will obviously have an effect on the porosity of the core, although this is expected to be minor. This problem can probably be avoided if the tubes were modified so as to have a gauze support at the base. Grain loss was a greater problem during the imbibition experiment. The pure water used clearly dissolved some of the sandstone matrix and hence altered the matrix porosity and permeability. This problem could also be avoided by using a 'sandstone-saturated' aqueous solution. It should be noted that the less handling of the core there is, the less the potential for losses. This is relevant for both grain loss and volatile loss if the experiment is to be carried out gravimetrically.

The imbibition and hysteresis experiment clearly shows DNAPL has been trapped or by-passed in the water flooding experiment. It would appear that the smaller pores have retained DNAPL or that larger pores have lost continuity and connectivity. From this experiment it is not possible to determine which process is taking place as the distribution of DNAPL within the core is unknown. When DNAPL was flooded back into a given core, very similar final residual water concentrations were found. The implication of this is that in a spill-scenario the residual saturation in the saturated zone will not exceed the maximum after the first DNAPL flood. Further water flooding and DNAPL flooding loops are needed to confirm this.

Combining core flooding data from a separate study (Bloomfield et al, 1997) a relationship has also been established between residual DNAPL and initial water saturation, with a trend of decreasing DNAPL saturation for increasing water saturation (Figure 8). This is quite intuitive as air filled pores are entered at lower entry pressures than water filled pores. The relationship is clearly more complex and will also be strongly dependant on the pore structure. Huling and Weaver (1991) have indicated that DNAPL residual saturation within the unsaturated zone is approximately a third of that in the saturated zone.

A relationship between mean pore size (as calculated from mercury intrusion capillary pressure data) and residual DNAPL has also been found. Figure 9 shows that with increasing mean pore size we find increasing DNAPL saturation. The trend line fitted to the data (simple log function) implies that residual DNAPL saturation will reach a maximum of around 70% saturation for the biggest pore sizes (100-150 μm) in consolidated sandstone matrix material. This places considerable emphasis on the importance of aspect ratio in assessing the degree of residual DNAPL saturation. Here it appears that the pores are large in relation to the throats (high aspect ratio) as the larger pores seem more likely to retain DNAPL than the small pores. Further work needs to be carried out in order to confirm or refute this.

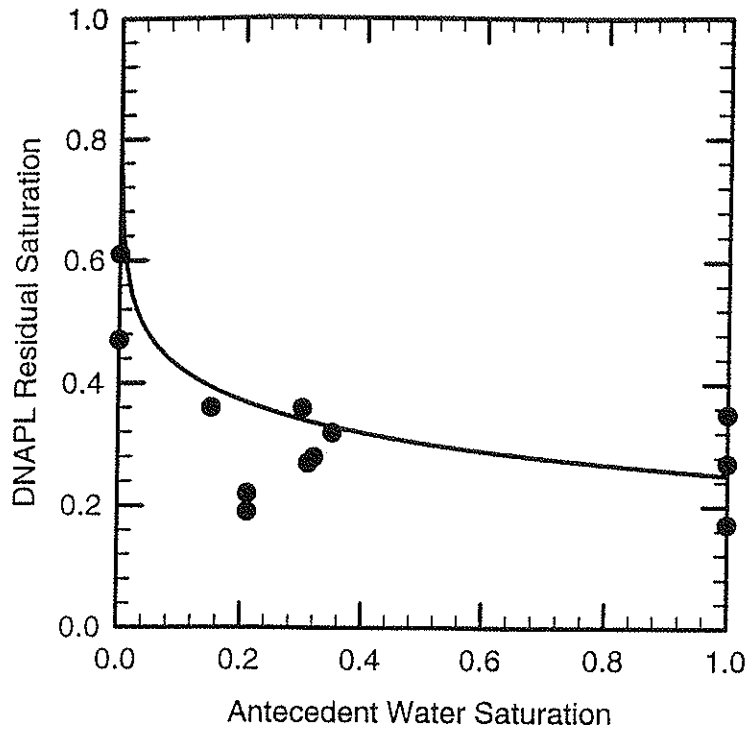


Figure 8. Relationship between residual DNAPL and antecedent water saturation

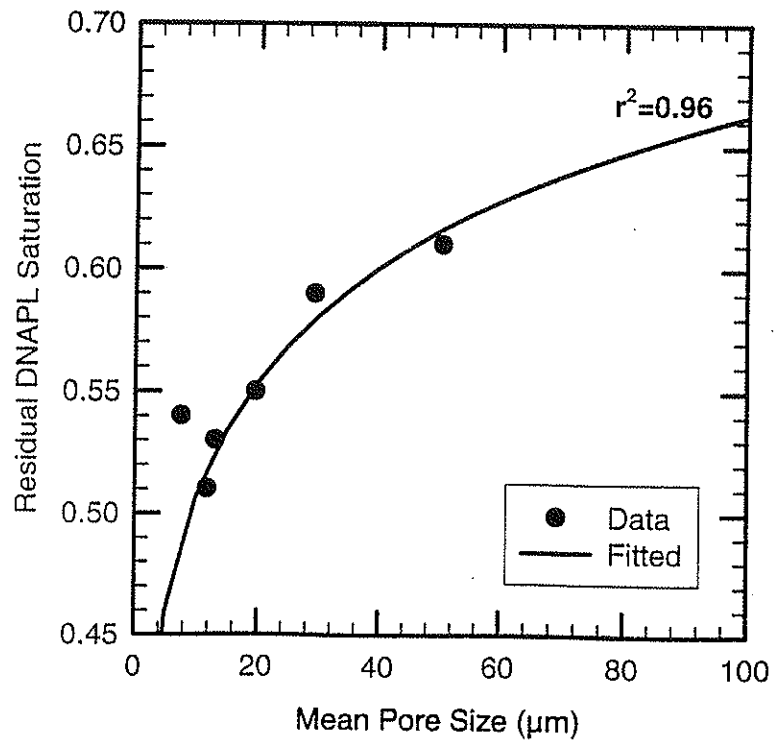


Figure 9. Residual DNAPL saturation as a function of mean pore size (μm)

6. REFERENCES

- Aurand K, Friesel P, Milde G and Neumayr V, 1981. Behaviour of organic solvents in the environment. *Studies in Environmental Science*, 12, 481-487.
- Bear J, 1988. *Dynamics of Fluids in Porous Media*, Dover Publishers, New York.
- Bloomfield J P, Goody D C and Williams A T, 1997. Laboratory measurements of chlorinated solvent residual saturation in the Helsby and Wilmslow Sandstones. British Geological Survey Technical Report Series WD/97/30C.
- Brooks R H and Corey A T, 1964. Hydraulic properties of porous media, Hydrology Paper no. 3, Colorado State University, Fort Collins, CO, 27 pp.
- Donaldson E C, Thomas R D and Lorenz P B, 1969. Wettability determination and its effect on recovery efficiency. *Society of Petroleum Engineering Journal*, March, 13-20.
- Hagoort J, 1980. Oil recovery by gravity damage. *SPEJ, Society of Petroleum Engineering Journal*, 20, 139-150
- Hassler G L and Brunner E, 1945. Measurement of capillary pressures in small core samples. *Trans. Am. Inst. Min. Metall. Eng.*, 160, 114-123.
- Hoffman R N, 1963. A technique for the determination of capillary pressure curves using a constantly accelerated centrifuge. *Society of Petroleum Engineers Journal*, 3, 227-235.
- Huling S G and Weaver J W, 1991. Dense nonaqueous phase liquids. USEPA/540/4-91/002, Robert S. Kerr Environmental Research Laboratory, Ada, Oklahoma.
- Kantzas A, Nikakhtar B, Ruth D and Pow M, 1995. Two phase relative permeabilities using the ultracentrifuge. *The Journal of Canadian Petroleum Technology*, 34, 7, 58-63.
- Keuper B H and Frind E O, 1991. Two-phase flow in heterogeneous porous media, 1. Model development. *Water Resources Research*, 27(6), 1049-1058
- Kinniburgh D G and Miles D L, 1983. Extraction and chemical analysis of interstitial water from soils and rocks. *Environmental Science and Technology*, 17, 362-368.
- Marx J W, 1956. Determining gravity drainage characteristics on the centrifuge. *Trans. Am. Inst. Min., Metall. Pet. Eng.*, 207, 88-91.
- Nikakhtar B, Kantzas A, De Wit P, Pow M and George A, 1996. On the characterising of Rock/Fluid and Fluid/Fluid Interactions in Carbonate Rocks Using the Ultracentrifuge. *The Journal of Canadian Petroleum Technology*, 35, 1, 47-56.
- Parker J C, 1989. Multiphase flow and transport in porous media. *Review Geophysics AGU*, 27(3), 311-328.
- Ruth D and Wong S, 1990. Centrifuge capillary pressure curves. *The Journal of Canadian Petroleum Technology*, 29,37, 67-72.

- Samaroo B H and Guerrero E T, 1981. The effect of temperature on drainage capillary pressure in rocks using a modified centrifuge. *SPE Paper 10153, Annual Fall Technical Conference of the Society of Petroleum Engineers AIME, 56th.*
- Slobod RL and Chambers A, 1951. Use of centrifuge for determining connate water, residual water, and capillary pressure curves of small core samples. *Trans. AIME, 192, 127-134.*
- Szabo M T, 1970. New methods for measuring the imbibition capillary pressure and electrical resistivity curves by centrifuge. *SPE Paper 3038, Annual Fall Technical Conference of the Society of Petroleum Engineers AIME, 45th.*
- van Genuchten, M Th, 1980. A closed form equation for predicting the hydraulic conductivity of unsaturated soils. *Soil Science Society of America Journal, 44, 892-898.*
- Van Spronsen E, 1982. Three-phase relative permeability measurements using the centrifuge method. *SPE/DOE Paper 10688, Joint Symposium on Enhanced Oil Recovery, 3rd.*
- Wilson J L, Conrad S H, Mason W R, Peplinski W and Hagen E, 1990. Laboratory investigation of residual liquid organics. USEPA/600/6-90/004, Robert S. Kerr Environmental Research Laboratory, Ada, Oklahoma, 267pp